

Electronic Supporting Information

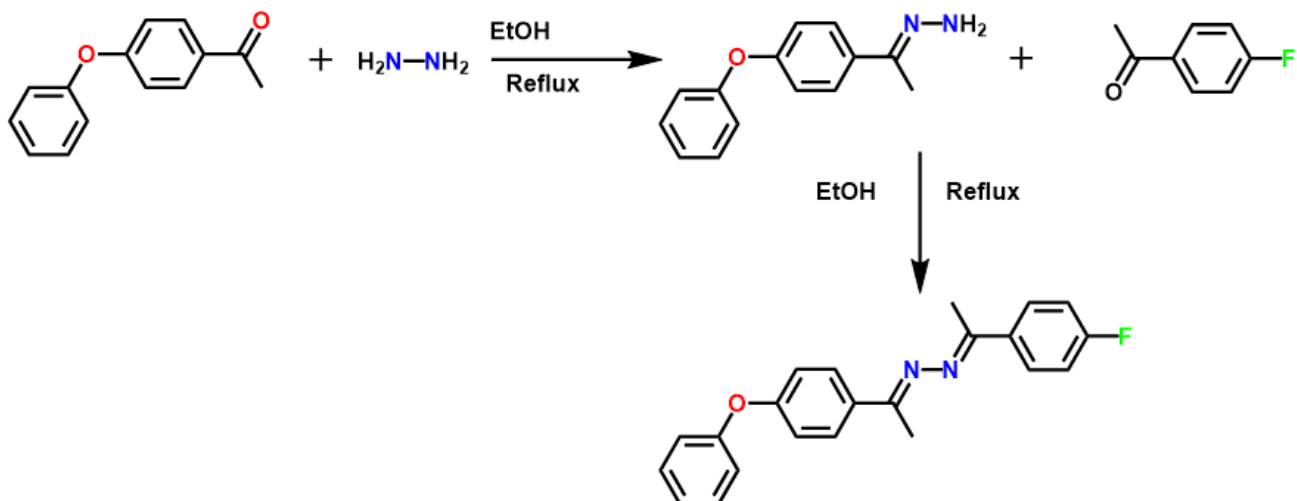
Polar and non-polar stacking of perfectly aligned parallel beloamphiphile monolayers (PBAMs) of (PhO, F)-azine. The interplay of non-covalent interlayer interactions and unit cell polarity

Harmeet Bhoday, Steven P. Kelley and Rainer Glaser*

Table of Contents

Experimental Section	S2-S8
Scheme S1 Two-step synthesis of (PhO, F)-azine from p-phenoxyacetophenone and p-fluoroacetophenone.....	S2
Fig. S1 Images of the crude (PhO, F)-azine product and its polymorphs I and II	S2
Table S1 Crystal parameters of various polymorphic forms of I and II	S3
Table S2 Parameters used for the GC/MS analyses of (PhO, F)-azine.....	S4
Fig. S2 GC trace (top) and mass spectrum (bottom) of pure (PhO, F)-azine	S4
Fig. S3 ¹ H-NMR spectrum of pure (PhO, F)-azine in CDCl ₃	S5
Fig. S4 ¹⁹ F-NMR spectrum of pure (PhO, F)-azine in CDCl ₃	S6
Fig. S5 ¹³ C-NMR spectrum of pure (PhO, F)-azine in CDCl ₃	S7
Fig. S6 FTIR spectrum of pure (PhO, F)-azine: calculated in gas-phase and ATR-FTIR spectra for I and II	S8
Molecular Geometry Data for Polymorphic Forms I and II	S9-S14
Fig. S7 Helicities exemplified for I	S9
Fig. S8 Helicities of molecules in the unit cells for I and II	S10
Fig. S9 Atom numbering for I-A in the crystal structure of I	S11
Table S3 Bond Lengths in I and II	S12
Table S4 Bond Angles in I and II	S13
Table S5 Torsions/Dihedrals in I and II	S14
Comparative Analysis of PBAM Structures	S15-S22
Fig. S10 PBAMs overlay of I and II	S15
Fig. S11 Hirshfeld surfaces for the molecules A and B of form I	S16
Fig. S12 Hirshfeld surfaces for the form II and (PhO, Cl)-azine	S17
Fig. S13 Complete Hirshfeld fingerprint plots for molecules I-A , I-B , and II-A in polymorphs I and II	S18
Fig. S14 Hirshfeld fingerprint plots for forms I-A , I-B , and II	S19
Fig. S15 Hirshfeld fingerprint plots for II and (PhO, Cl)-azine	S20
Fig. S16 Molecular packing shells in I and II	S21
Table S6 Favorable <i>intralayer</i> interactions in I	S22
Table S7 Favorable <i>intralayer</i> interactions in II	S23
Pairwise Interaction Energies	S24
Fig. S17 Color-coded interaction mapping within 3.8 Å of A * in I	S24
Table S8 Color-coded pairwise interaction energies relative to A * in I	S24
Fig. S18 Color-coded interaction mapping within 3.8 Å of B * in I	S25
Table S9 Color-coded pairwise interaction energies relative to B * in I	S25
Fig. S19 Color-coded interaction mapping within 3.8 Å of A * in II	S25
Table S10 Color-coded pairwise interaction energies relative to A * in II	S25
Lattice Energy Calculations for Polymorph I and II	S26
Fig. S20 Molecular packing shell for I used in CrystalExplorer.....	S26

Experimental Section



Scheme S1 Two-step synthesis of (PhO, F)-azine from p-phenoxyacetophenone and p-fluoroacetophenone.

Synthetic Procedure and Characterization: The synthesis of (PhO, F)-azine involved two steps. In the first step, 5.6 mmol (1.2 g) of the p-phenoxyacetophenone (MW = 212.24 g/mol) was added to a 100 ml round-bottomed flask followed by addition of 5.6 mmol (0.28 ml) hydrazine hydrate (64% w/w), 3-4 drops of glacial acetic acid (catalyst) and 15 ml ethanol (solvent). The reaction mixture was refluxed at 78-80 °C for 4 hours and the progress of the reaction was monitored by TLC using n-hexane:ethyl acetate eluents (95:5). The reaction was assumed to be complete when the reactant spot on TLC was invisible. In the second step, 60 ml ethanol was first added and then 1.6 mmol (ml) of p-fluoroacetophenone was added. The mixture was refluxed for 24 hours at 78-80 °C until the reactant spots are faintly visible or completely invisible. Finally, the reaction mixture was concentrated by evaporation of ethanol (water condenser was removed to avoid condensation) to allow for precipitation of the product. The yellow colored product separates out of solution when the mixture cools down to room temperature. The crude product was filtered off and vacuum dried. The purity of the product was examined using TLC using n-hexane:ethyl acetate eluents in 95:5 ratio and the same is shown in **Fig. S1**. **¹H-NMR** (400 MHz, CDCl_3) δ 7.90 – 7.86 (m, 4H), 7.37 - 7.31 (t, 2H), 7.14 - 7.00 (m, 7H), 2.31 (s, 6H). **¹³C-NMR** (100 MHz, CDCl_3) δ 163.8, 159.16, 156.81, 134.6, 133.3 130.08, 128.80, 128.71, 128.51, 119.64, 118.36, 115.60, 115.38, 15.17. **¹⁹F-NMR** (375 MHz, CDCl_3 , proton-decoupled) δ -111.59. **MS** m/z: $[\text{C}_{22}\text{H}_{19}\text{FN}_2\text{O}]^+$, 346 (MW = 346.15); base peak, 331.

Crystallization: Crystals of the size 0.2-0.3 mm were grown from the pure (PhO, F)-azine sample using various solvents (acetone, chloroform, ethyl acetate/hexane mix., ethanol, toluene) via slow evaporation technique. Ethyl acetate/hexane mix, ethanol and Toluene resulted in better quality crystals. Polymorph **I** (antiferroelectric) results from a crystallization with ethyl acetate/hexane (1:10) mixture while pure toluene and ethanol favor the formation of Polymorph **II** (ferroelectric). The vials were covered using paraffin film with a few holes and kept in the fumehood at room temperature without any mechanical disturbance for a week or more until crystals appeared.

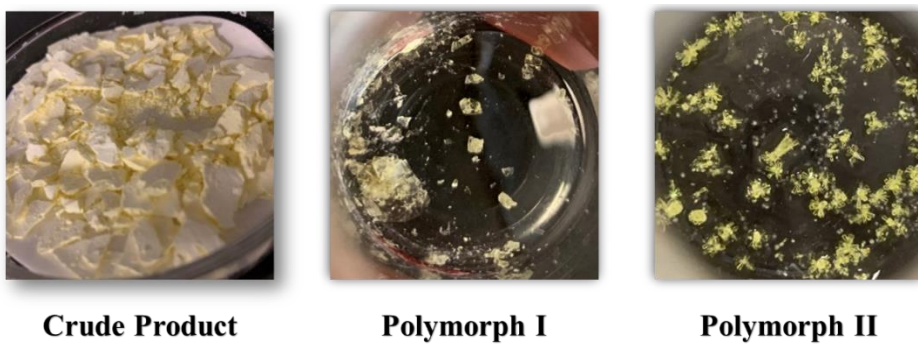


Fig. S1 Images of the crude (PhO, F)-azine product and its polymorphs **I** and **II**.

Table S1 Crystal parameters of various polymorphic forms of **I** and **II**.

(PhO, F)-azine	Form Ia ^a	Form Ib ^a	Form IIa ^b	Form IIb ^b
Crystal system	Triclinic	Triclinic	Orthorhombic	Orthorhombic
Space group	P $\bar{1}$	P $\bar{1}$	Pna2 ₁	Pna2 ₁
a/ \AA	6.5410(2)	6.5322(15)	6.5339(3)	6.5274(3)
b/ \AA	7.1465(2)	7.3486(17)	7.1569(3)	7.2009(3)
c/ \AA	37.8014(10)	37.987(9)	37.6943(15)	37.7553(16)
$\alpha/^\circ$	91.0820(12)	91.159(3)	90	90
$\beta/^\circ$	94.0970(12)	93.956(3)	90	90
$\gamma/^\circ$	90.1522(13)	90.147(4)	90	90
V/ \AA^3	1762.19(9)	1818.7(7)	1762.68(13)	1774.62(13)
Z/Z'	4/2	4/2	4/1	4/1
T/K	100	293	100	150
RI [$I > 2\sigma(I)$]	0.0579	0.0699	0.0428	0.0278
wR2 (all)	0.1644	0.1995	0.1168	0.0783
Goodness-of-fit	1.197	0.920	1.083	1.064

^a Reflections for polymorph **I** recorded at 100 K (**Ia**) and 293 K (**Ib**)^b Reflections for polymorph **II** recorded at 100 K (**IIa**) and 150 K (**IIb**)

Table S2 Parameters used for the GC/MS analyses of (PhO, F)-azine.

Column Oven Temp. :100.0 °C	SPL Purge : Yes
Injection Temp. :320.00 °C	< Ready Check APC Flow > < Ready
Injection Mode :Split	Check Detector APC Flow >
Flow Control Mode :Pressure	External Wait :No
Pressure :100.0 kPa	Equilibrium Time :0.1 min
Total Flow :17.7 mL/min	[GC Program]
Column Flow :1.33 mL/min	[GCMS-QP2020]
Linear Velocity :43.0 cm/sec	Ion Source Temp :200.00 °C
Purge Flow :3.0 mL/min	Interface Temp. :320.00 °C
Split Ratio :10.0	Solvent Cut Time :2.00 min
High Pressure Injection :OFF	Detector Gain Mode :Relative to the
Carrier Gas Saver :ON	Tuning Result
Carrier Gas Saver Split Ratio :1.0	Detector Gain :0.82 kV +0.00 kV
Carrier Gas Saver Time :1.00 min	Threshold :0
Splitter Hold :OFF	[MS Table]
Oven Temp. Program	--Group 1 - Event 1--
Rate Temperature(°C) Hold Time(min)	Start Time :2.10min
- 100.0 2.00	End Time :16.00min
20.00 320.0 3.00	ACQ Mode :Scan
< Ready Check Heat Unit >	Event Time :0.05sec
Column Oven : Yes	Scan Speed :10000
SPL : Yes	Start m/z :10.00
MS : Yes	End m/z :420.00
< Ready Check Detector(FTD/BID) >	Sample Inlet Unit :GC
< Ready Check Baseline Drift >	[MS Program]
SPL Carrier : Yes	Use MS Program :OFF

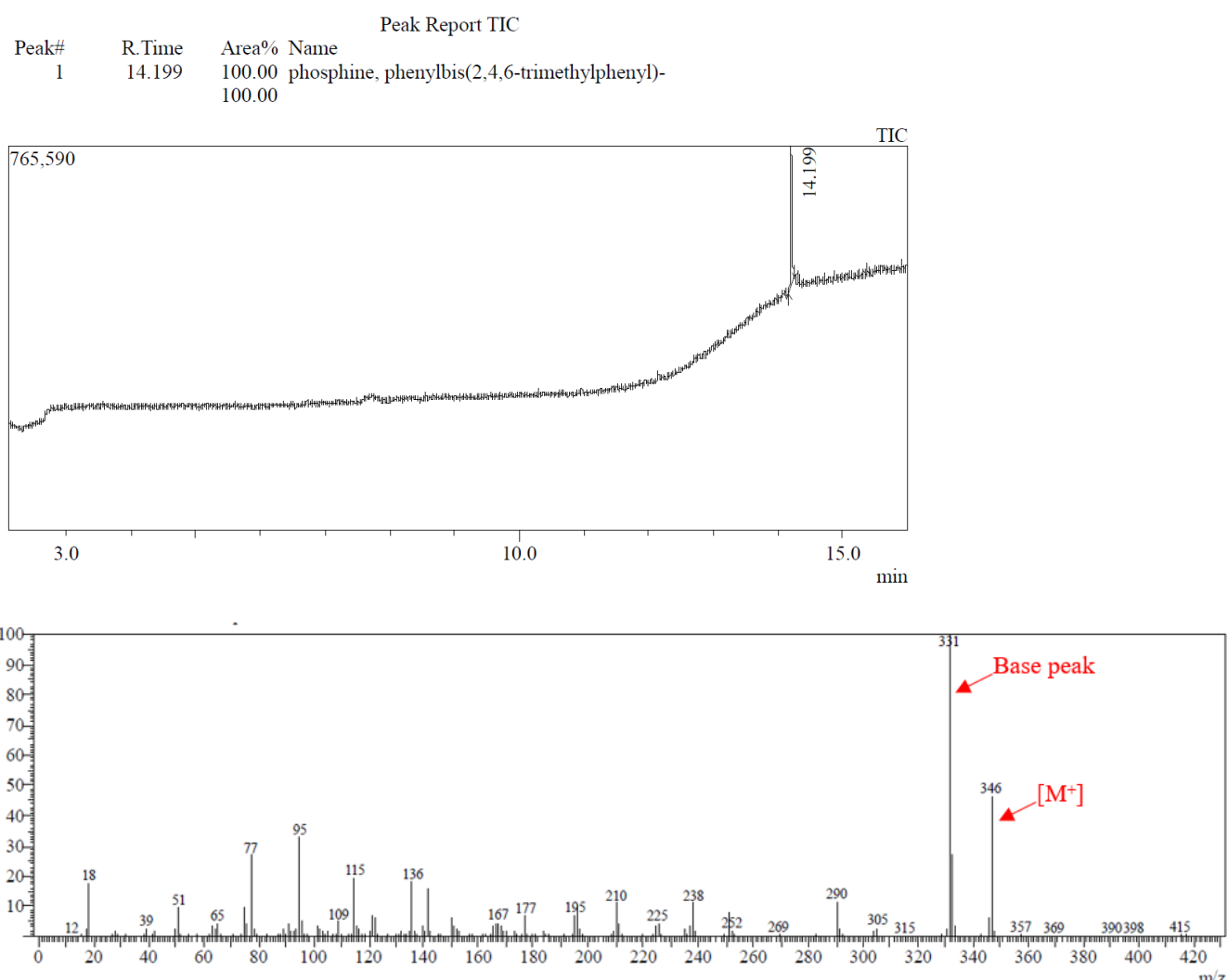


Fig. S2 GC trace (top) and mass spectrum (bottom) of pure (PhO, F)-azine (molecular mass = 346.40 a.u.).

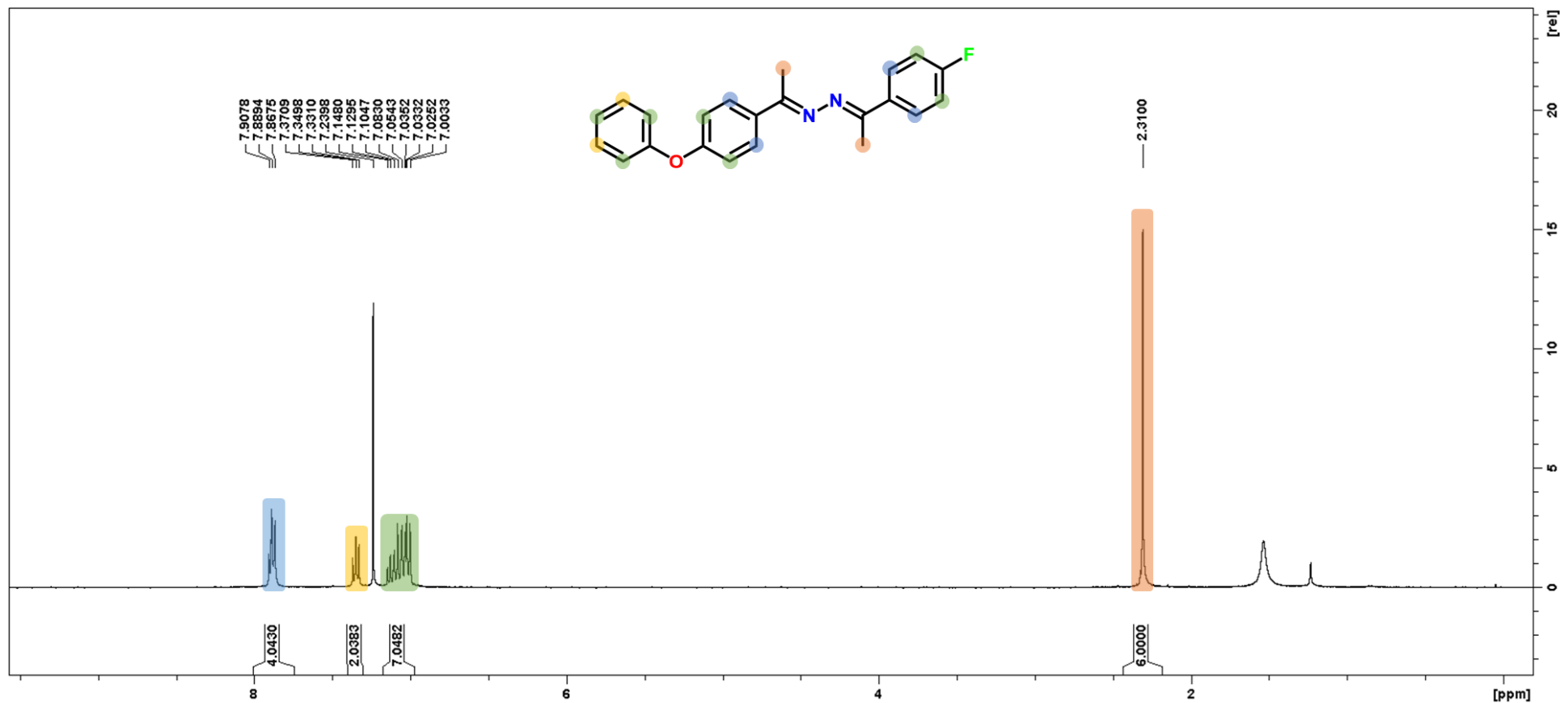


Fig. S3 ^1H -NMR spectrum of pure (PhO, F)-azine in CDCl_3 .

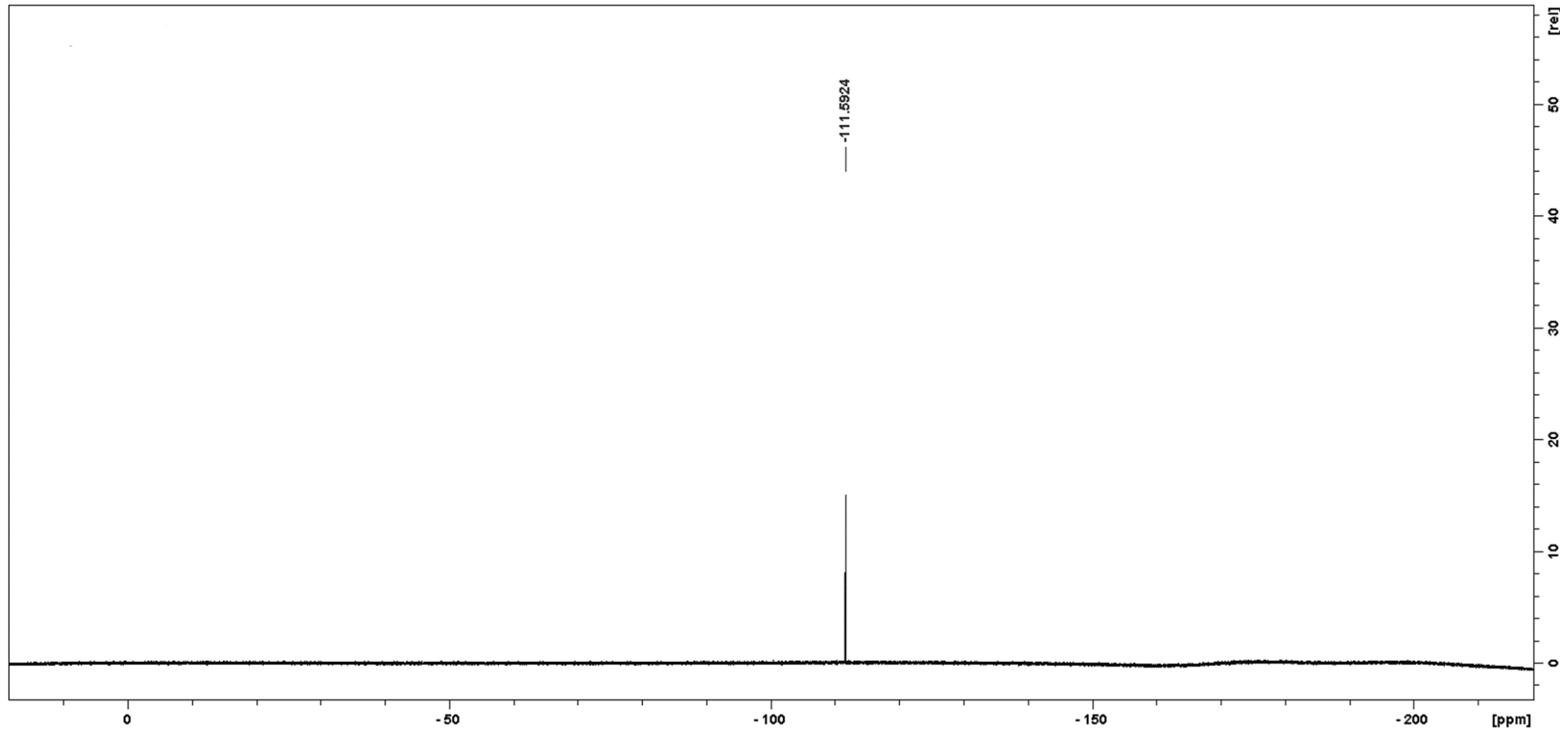


Fig. S4 ${}^{19}\text{F}$ -NMR (proton-decoupled) spectrum of pure (PhO, F)-azine in CDCl_3 .

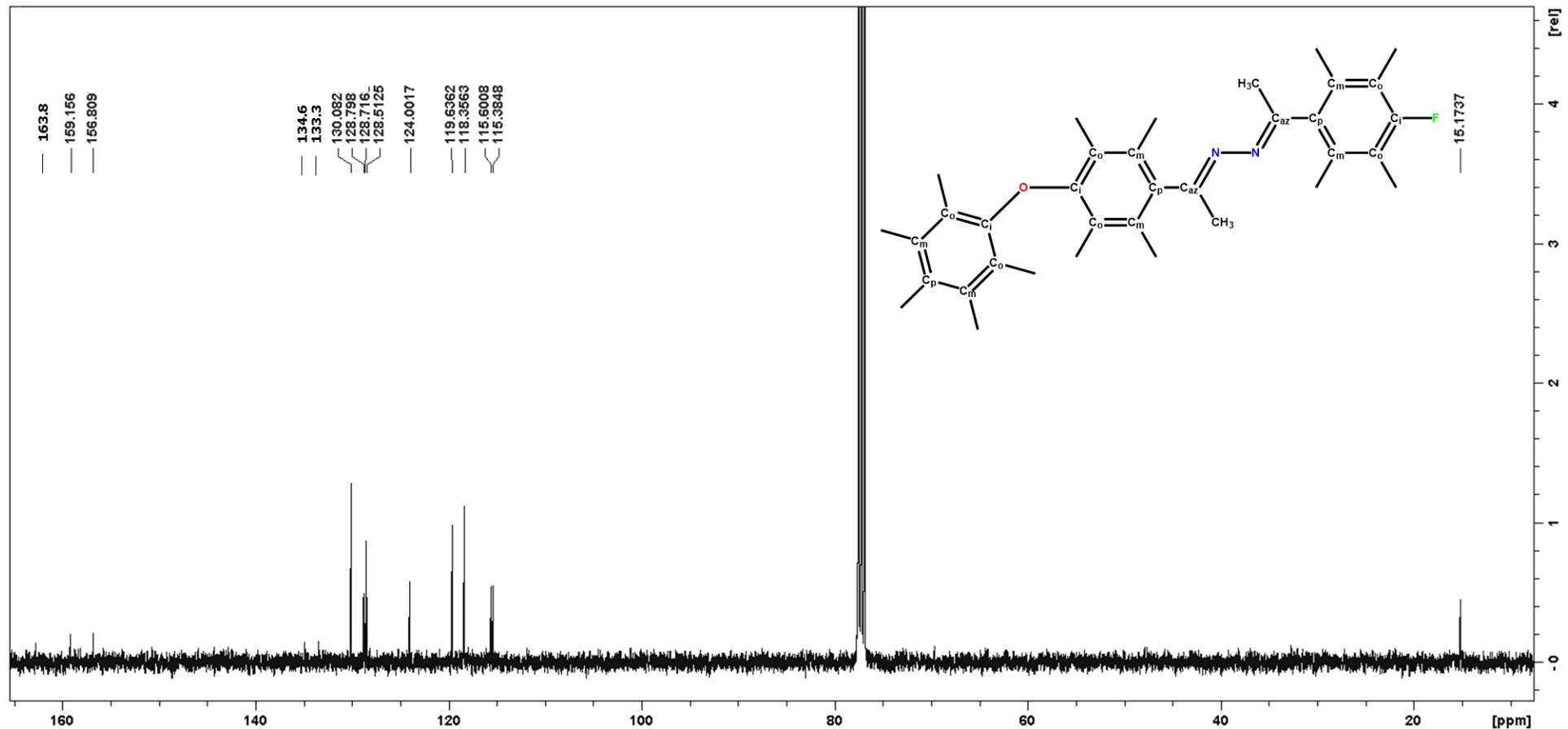


Fig. S5 ^{13}C -NMR spectrum of pure (PhO, F)-azine in CDCl_3 .

C _I	C _O	C _M	C _P	C _{Az}	C _{H3}	'C _{H3}	C _{Az'}	C _{P'}	C _{M'}	C _{O'}	C _{I'}
158.9	119.4	129.8	133.3	157.9	14.9	14.9	157.3	134.6	128.5	115.3	163.8

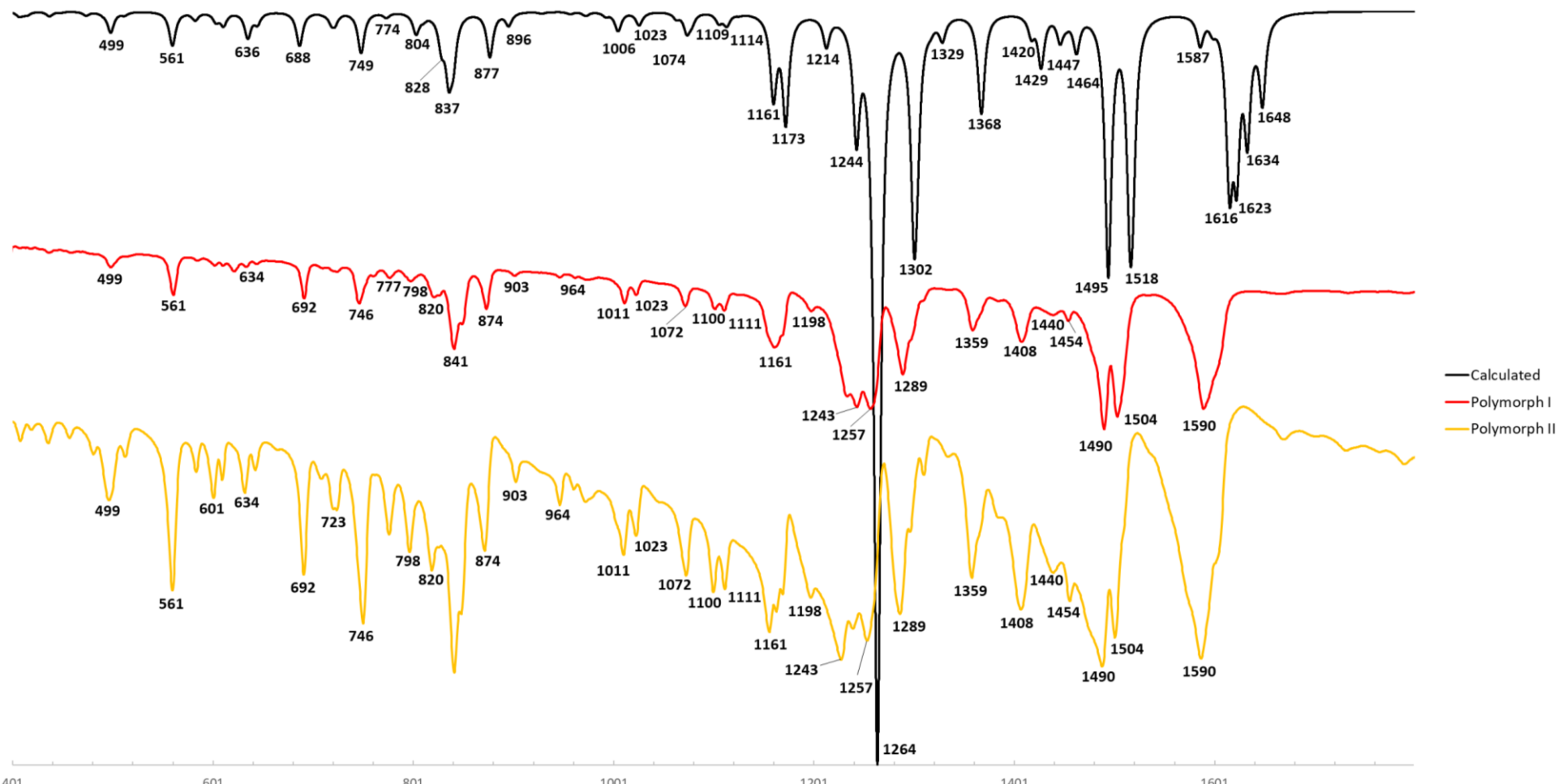


Fig. S6 FTIR spectrum of pure (PhO, F)-azine: Calculated for gas-phase at APFD/6-311G* level (top) and ATR-FTIR spectra for polymorph I (middle), polymorph II (bottom).

Molecular Geometry data for polymorphic forms I and II

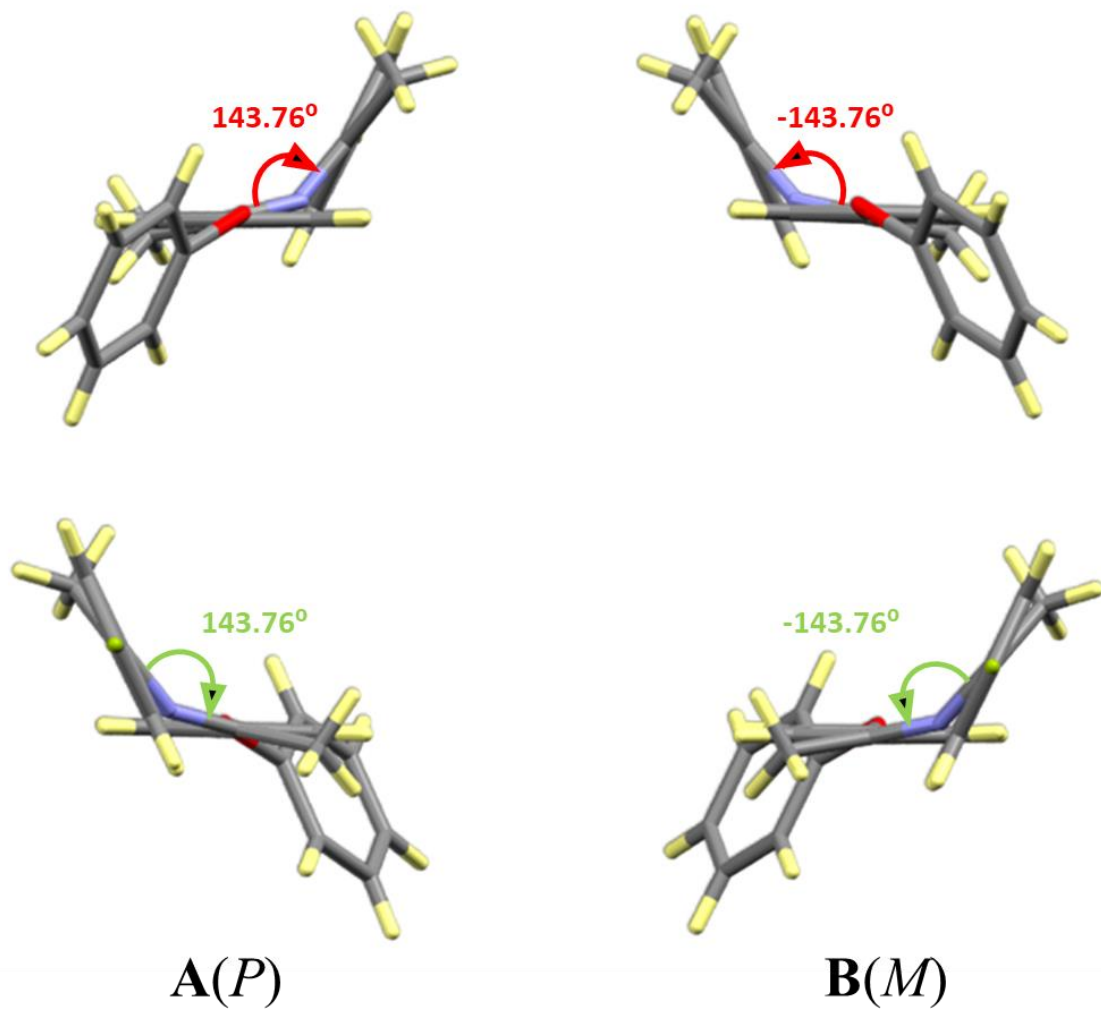


Fig. S7 Independent molecules **A** and **B** of **I** exemplify *P* and *M* helicities, respectively. Newman projections are shown down the N—N axis with the phenoxy group in front (top) or in back (bottom). The helicity does not depend on the molecule orientation.

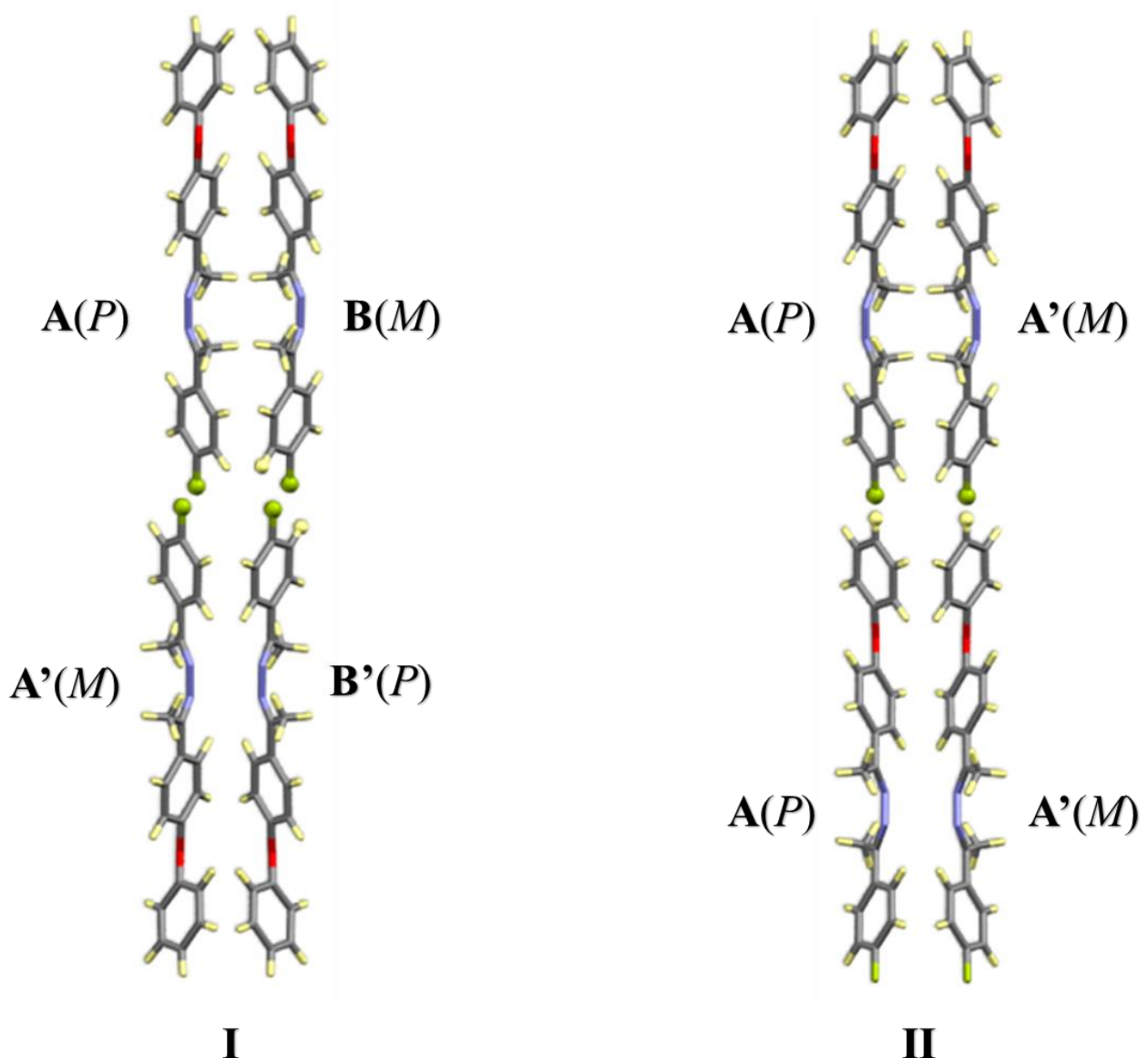


Fig. S8 Helicities of molecules in the unit cells for **I** and **II**. Enantiomers are indicated by a superscripted prime ('), i.e., **A'** is the enantiomer of **A**.

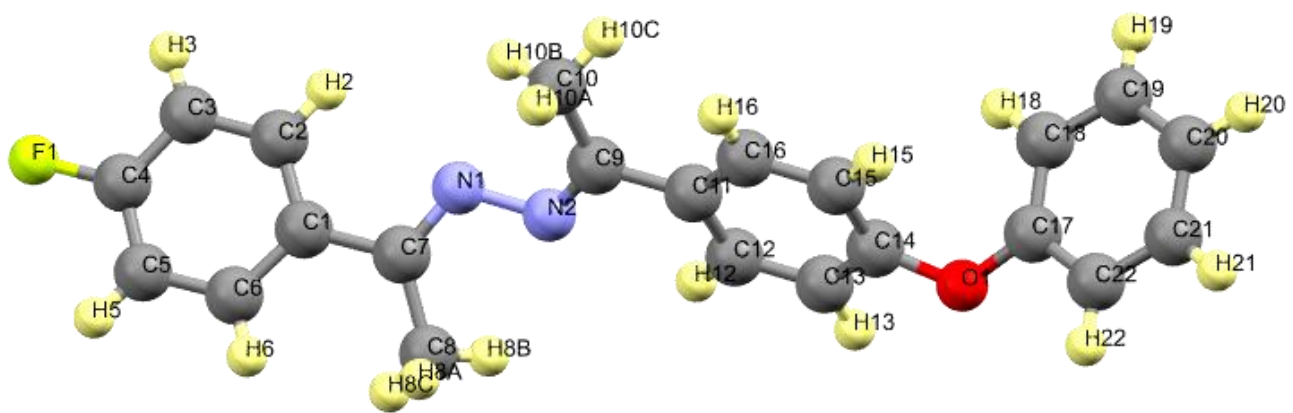


Fig. S9 Atom numbering for **I-A** in the crystal structure of **I**.

Table S3 Bond Lengths (\AA) in **I** (100 K) and **II** (100 K). The atom numbering used for the crystal of **I-A** is employed in this table for all molecules.^{a-c}

Atom 1	Atom 2	I-A	esd (I-A)	I-B	esd (I-B)	II-A	esd (II-A)	Average esd	Average	Std. dev.
F1	C4	1.355	0.003	1.356	0.003	1.355	0.002	0.003	1.355	0.000
O1	C14	1.386	0.003	1.385	0.003	1.377	0.003	0.003	1.383	0.004
O1	C17	1.390	0.003	1.392	0.003	1.394	0.003	0.003	1.392	0.002
N1	N2	1.393	0.003	1.394	0.003	1.394	0.002	0.003	1.394	0.000
N1	C7	1.285	0.003	1.282	0.003	1.286	0.003	0.003	1.284	0.002
N2	C9	1.289	0.003	1.288	0.003	1.293	0.003	0.003	1.290	0.002
C1	C2	1.397	0.003	1.404	0.003	1.404	0.003	0.003	1.402	0.003
C1	C6	1.397	0.003	1.397	0.003	1.400	0.003	0.003	1.398	0.001
C1	C7	1.489	0.003	1.484	0.003	1.485	0.003	0.003	1.486	0.002
C2	C3	1.387	0.003	1.387	0.003	1.392	0.003	0.003	1.389	0.002
C3	C4	1.385	0.003	1.382	0.003	1.383	0.003	0.003	1.383	0.001
C4	C5	1.374	0.003	1.372	0.003	1.379	0.003	0.003	1.375	0.003
C5	C6	1.391	0.003	1.391	0.003	1.394	0.003	0.003	1.392	0.001
C7	C8	1.503	0.003	1.508	0.003	1.497	0.003	0.003	1.503	0.004
C9	C10	1.497	0.003	1.495	0.003	1.496	0.003	0.003	1.496	0.001
C9	C11	1.488	0.003	1.486	0.003	1.480	0.003	0.003	1.485	0.003
C11	C12	1.406	0.003	1.400	0.003	1.406	0.003	0.003	1.404	0.003
C11	C16	1.396	0.003	1.401	0.003	1.402	0.003	0.003	1.400	0.003
C12	C13	1.382	0.003	1.393	0.003	1.383	0.003	0.003	1.386	0.005
C13	C14	1.390	0.003	1.389	0.003	1.395	0.003	0.003	1.391	0.003
C14	C15	1.387	0.003	1.394	0.003	1.398	0.003	0.003	1.393	0.005
C15	C16	1.396	0.003	1.383	0.003	1.391	0.003	0.003	1.390	0.005
C17	C18	1.394	0.003	1.391	0.003	1.384	0.003	0.003	1.390	0.004
C17	C22	1.383	0.003	1.388	0.003	1.387	0.003	0.003	1.386	0.002
C18	C19	1.395	0.003	1.390	0.003	1.399	0.003	0.003	1.395	0.004
C19	C20	1.389	0.003	1.392	0.003	1.390	0.003	0.003	1.390	0.001
C20	C21	1.389	0.003	1.385	0.003	1.386	0.003	0.003	1.387	0.002
C21	C22	1.388	0.003	1.394	0.003	1.394	0.003	0.003	1.392	0.003

^a Bond lengths are given along with estimated standard deviations (e.s.d.).

^b In columns “Average” and “Std. dev.” the average bond lengths in molecules **I-A**, **I-B** and **II** are given along with their standard deviations.

^c The molecular structures are virtually identical with standard deviations not exceeding average e.s.d. values.

Table S4 Bond Angles (\AA) in **I** (100 K) and **II** (100 K). The atom numbering used for the crystal of **I-A** is employed in this table for all molecules.^{a-c}

Atom 1	Atom 2	Atom 3	I-A	esd (I-A)	I-B	esd (I-B)	II-A	esd (I-C)	Average esd	Average	Std. dev.
C14	O1	C17	120.85	0.17	120.58	0.17	121.02	0.16	0.17	120.82	0.18
C7	N1	N2	114.46	0.19	114.60	0.19	114.53	0.18	0.19	114.53	0.06
C9	N2	N1	115.10	0.19	114.83	0.19	115.12	0.18	0.19	115.02	0.13
C2	C1	C6	118.40	0.20	118.40	0.20	118.32	0.19	0.20	118.37	0.04
C2	C1	C7	120.60	0.20	120.10	0.20	120.22	0.19	0.20	120.31	0.21
C6	C1	C7	121.00	0.20	121.40	0.20	121.45	0.19	0.20	121.28	0.20
C3	C2	C1	121.30	0.20	121.00	0.20	121.07	0.19	0.20	121.12	0.13
C4	C3	C2	118.20	0.20	118.20	0.20	118.30	0.20	0.20	118.23	0.05
F1	C4	C3	118.50	0.20	118.30	0.20	118.50	0.20	0.20	118.43	0.09
F1	C4	C5	118.80	0.20	118.80	0.20	118.70	0.20	0.20	118.77	0.05
C5	C4	C3	122.70	0.20	122.90	0.20	122.80	0.20	0.20	122.80	0.08
C4	C5	C6	118.30	0.20	118.40	0.20	118.20	0.20	0.20	118.30	0.08
C5	C6	C1	121.20	0.20	121.00	0.20	121.30	0.20	0.20	121.17	0.12
N1	C7	C1	116.70	0.20	116.50	0.20	116.08	0.19	0.20	116.43	0.26
N1	C7	C8	124.00	0.20	124.00	0.20	124.10	0.20	0.20	124.03	0.05
C1	C7	C8	119.30	0.20	119.50	0.20	119.80	0.19	0.20	119.53	0.21
N2	C9	C10	124.20	0.20	124.20	0.20	123.90	0.20	0.20	124.10	0.14
N2	C9	C11	115.90	0.20	115.80	0.20	116.05	0.19	0.20	115.92	0.10
C11	C9	C10	119.90	0.20	119.94	0.19	120.06	0.19	0.19	119.97	0.07
C12	C11	C9	120.30	0.20	120.40	0.20	120.59	0.19	0.20	120.43	0.12
C16	C11	C9	121.50	0.20	121.50	0.20	121.34	0.19	0.20	121.45	0.08
C16	C11	C12	118.20	0.20	118.10	0.20	118.10	0.20	0.20	118.13	0.05
C13	C12	C11	120.80	0.20	121.30	0.20	121.16	0.19	0.20	121.09	0.21
C12	C13	C14	119.90	0.20	119.40	0.20	119.76	0.19	0.20	119.69	0.21
O1	C14	C13	115.40	0.20	115.15	0.19	115.63	0.19	0.19	115.39	0.20
O1	C14	C15	123.80	0.20	123.70	0.20	123.77	0.19	0.20	123.76	0.04
C15	C14	C13	120.60	0.20	120.90	0.20	120.50	0.20	0.20	120.67	0.17
C14	C15	C16	119.20	0.20	118.90	0.20	119.09	0.19	0.20	119.06	0.12
C15	C16	C11	121.20	0.20	121.40	0.20	121.50	0.20	0.20	121.37	0.12
O1	C17	C18	122.70	0.20	122.90	0.20	122.44	0.19	0.20	122.68	0.19
C22	C17	O1	115.58	0.19	115.30	0.20	115.47	0.20	0.20	115.45	0.12
C22	C17	C18	121.50	0.20	121.50	0.20	121.90	0.19	0.20	121.63	0.19
C17	C18	C19	118.50	0.20	118.80	0.20	118.70	0.20	0.20	118.67	0.12
C20	C19	C18	120.60	0.20	120.40	0.20	120.10	0.20	0.20	120.37	0.21
C19	C20	C21	119.70	0.20	119.90	0.20	120.10	0.20	0.20	119.90	0.16
C22	C21	C20	120.60	0.20	120.50	0.20	120.40	0.20	0.20	120.50	0.08
C17	C22	C21	119.10	0.20	118.80	0.20	118.70	0.20	0.20	118.87	0.17

^a Bond angles are given along with estimated standard deviations (e.s.d.).

^b In columns “Average” and “Std. dev.” the average bond angles in molecules **I-A**, **I-B** and **II** are given along with their standard deviations.

^c The molecular structures are virtually identical with standard deviations not exceeding average e.s.d. values.

Table S5 Torsions/Dihedrals in **I** (100 K) and **II** (100 K). The atom numbering used for the crystal of **I-A** is employed in this table for all molecules. Averaging occurs over molecules of the same helicity (*P*).^{a-d}

Atom 1	Atom 2	Atom 3	Atom 4	I-A ^d	esd (I-A)	I-B ^d	esd (I-B)	II-A	esd (I-C)	Average esd	Average	Std. dev.
C17	O1	C14	C13	150.5	0.2	150.6	0.2	151.2	0.2	0.2	150.8	0.3
C17	O1	C14	C15	-34.9	0.3	-34.7	0.3	-33.3	0.3	0.3	-34.3	0.7
C14	O1	C17	C18	-38.7	0.3	-39.1	0.3	-39.4	0.3	0.3	-39.1	0.3
C14	O1	C17	C22	146.8	0.2	146.0	0.2	145.9	0.2	0.2	146.2	0.4
C9	N2	N1	C7	-143.8	0.2	-143.8	0.2	-143.8	0.2	0.2	-143.8	0.0
C1	C7	N1	N2	-178.6	0.2	-179.2	0.2	-179.2	0.3	0.2	-179.0	0.3
C8	C7	N1	N2	2.4	0.3	2.1	0.3	2.3	0.3	0.3	2.3	0.1
C10	C9	N2	N1	2.0	0.3	2.0	0.3	2.2	0.3	0.3	2.1	0.1
C11	C9	N2	N1	-179.9	0.2	-179.7	0.2	-179.8	0.2	0.2	-179.8	0.1
C2	C1	C7	N1	13.3	0.3	15.3	0.3	14.1	0.3	0.3	14.2	0.8
C2	C1	C7	C8	-167.8	0.2	-167.5	0.2	-167.4	0.2	0.2	-167.6	0.2
C6	C1	C7	N1	-167.0	0.2	-165.9	0.2	-165.0	0.2	0.2	-166.0	0.8
C6	C1	C7	C8	12.0	0.3	15.0	0.3	13.5	0.3	0.3	13.5	1.2
C12	C11	C9	N2	12.2	0.3	11.6	0.3	12.2	0.3	0.3	12.0	0.3
C16	C11	C9	N2	-166.5	0.2	-167.5	0.2	-166.6	0.2	0.2	-166.9	0.4
C12	C11	C9	C10	-169.6	0.2	-170.8	0.2	-169.8	0.2	0.2	-170.1	0.5
C16	C11	C9	C10	11.7	0.3	10.2	0.3	11.4	0.3	0.3	11.1	0.6

^a Torsion angles are given along with estimated standard deviations (e.s.d.).

^b In columns “Average” and “Std. dev.” the average torsion angles in molecules **I-A**, **I-B** and **II** are given along with their standard deviations.

^c The molecular structures are virtually identical with standard deviations not exceeding average e.s.d. values.

^d Molecules **A** and **B** in **I** have opposite helicity. In the present table the dihedrals are shown for the independent molecules with *P* helicity.

Comparative Analysis of PBAM Structures

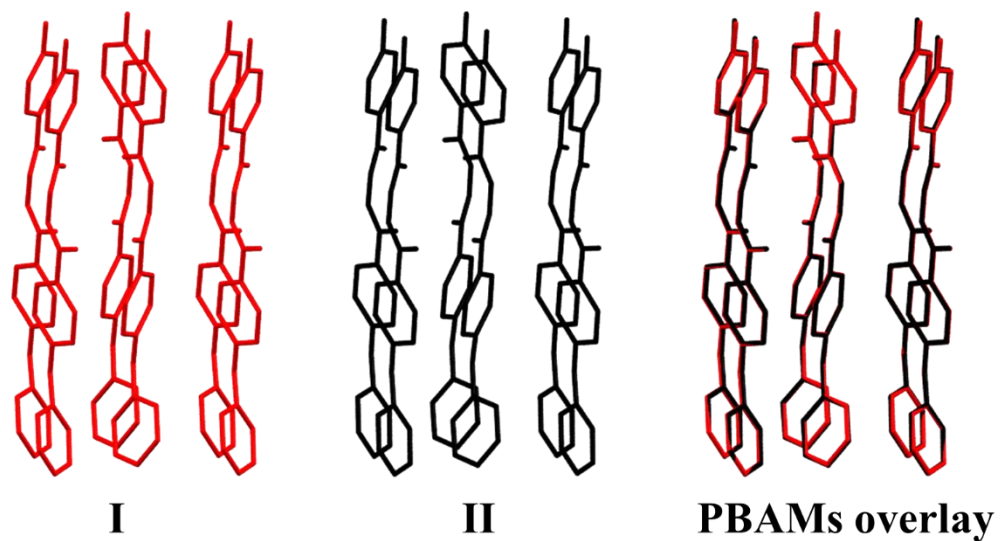
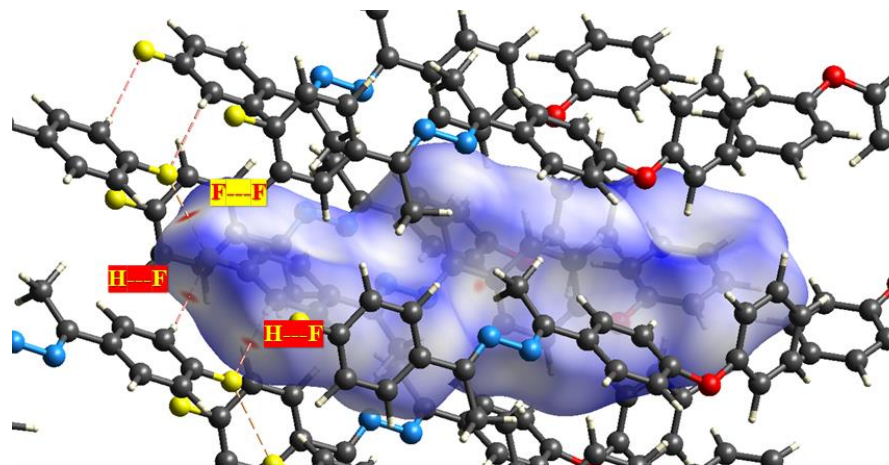
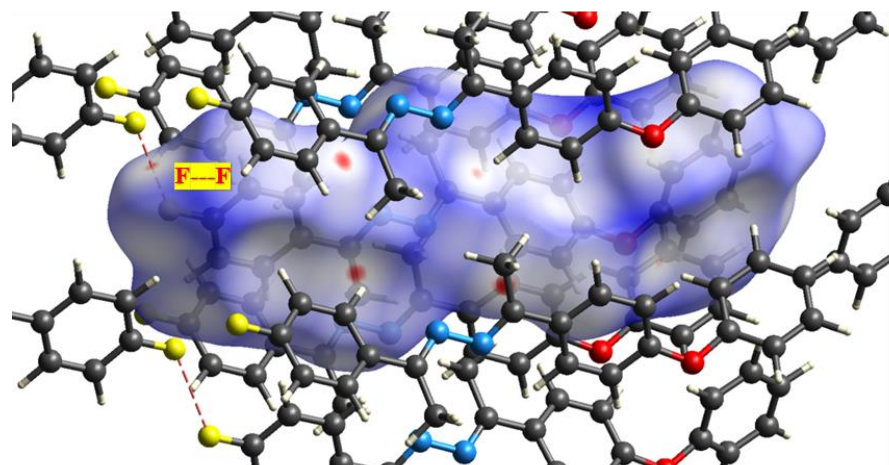
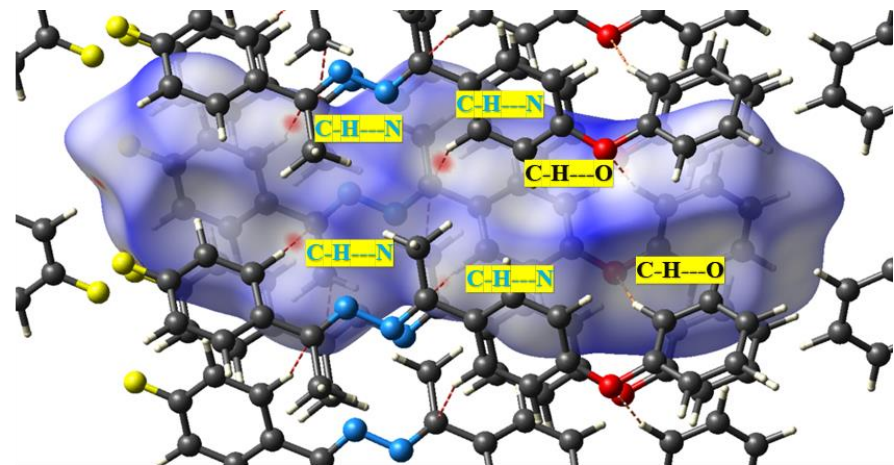


Fig. S10 Stick presentations of PBAMs of polymorph **I** (red), **II** (black) and their overlay, hydrogen atoms have been omitted for clarity. The PBAMs in both the polymorphs are only slightly different.



I-A



I-B

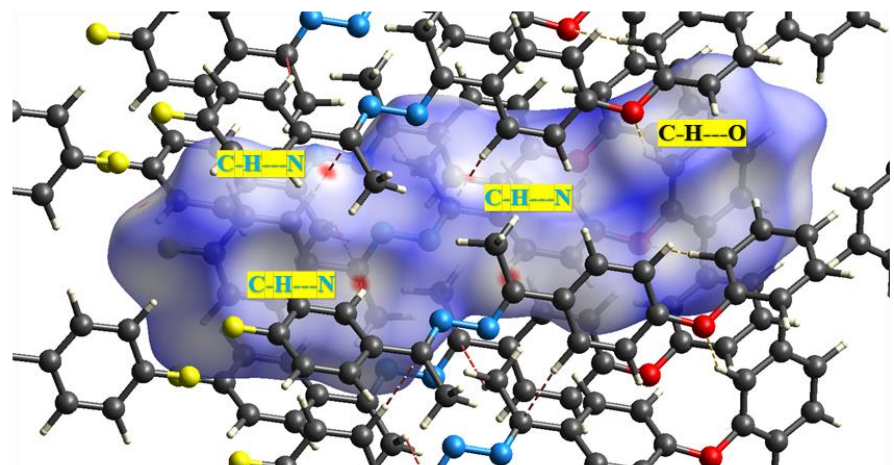


Fig. S11 Hirshfeld surfaces for the molecules **A** (top) and **B** (bottom) of **I**. The bluish domains indicate that the distance between neighboring atoms is larger than the sum of their respective van der Waals radii. The white areas define the places where the distance is close to the sum of the van der Waals radii of the considered atoms. The red color represents the places of significant interactions where the distance is less than the sum of the van der Waals radii. **A** and **B** do not feature much differences in the *intralayer* interactions (right) but the *interlayer* interactions are significantly different (left).

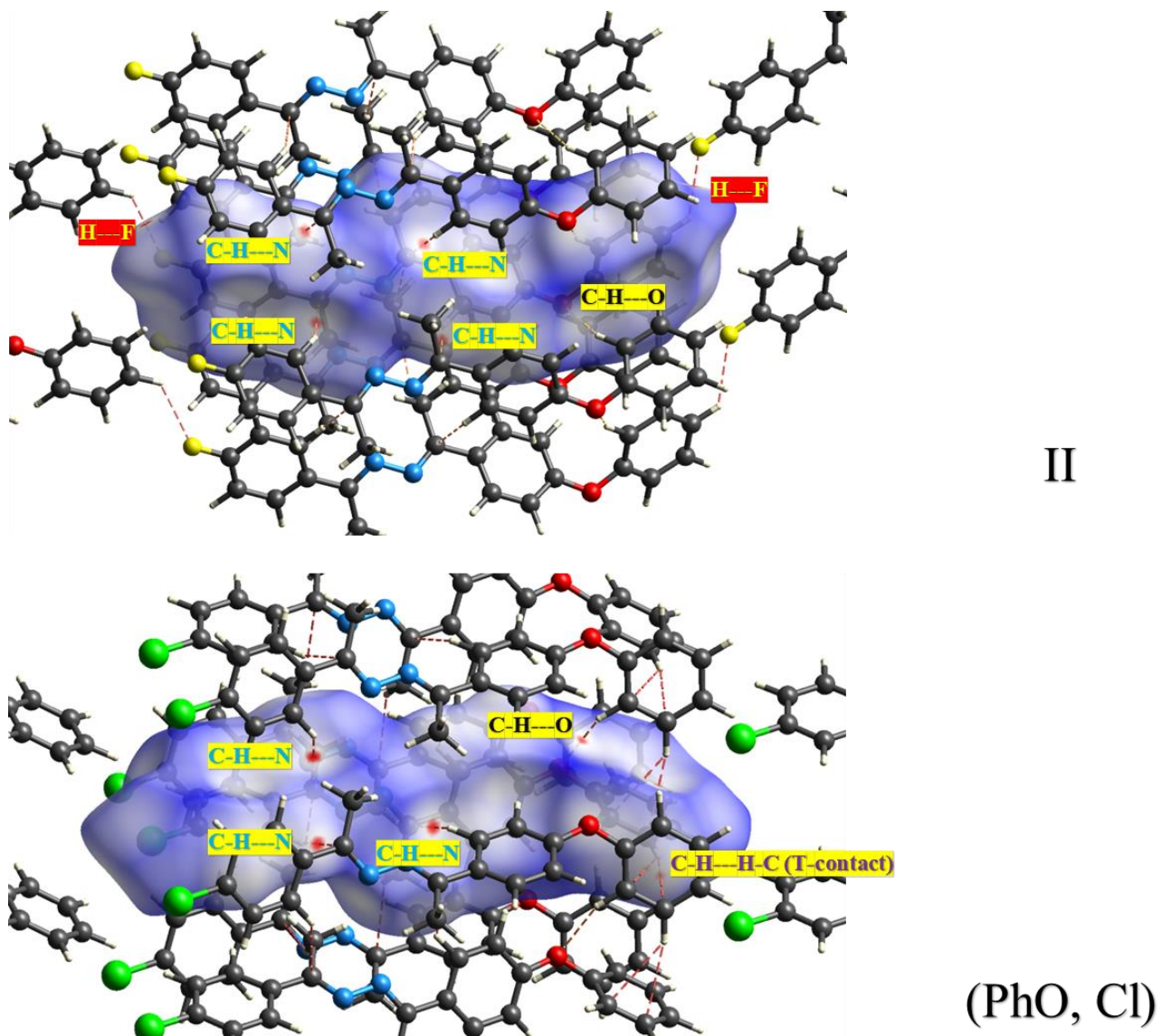


Fig. S12 Hirshfeld surfaces for the polymorph **II** of the (PhO, F)-azine (top) and (PhO, Cl)-azine (bottom). (PhO, F)-azine has directional C-H---F interactions at the F/PhO interface but no such interactions exist at the Cl/PhO interface. This explains why (PhO, F)-azine adapts a zigzag structure with a kink but the crystals of (PhO, Cl)-azine are perfectly parallel aligned. The Hirshfeld surfaces for other perfectly parallel aligned crystal structures of (PhO, Br)- and (PhO, I)-azine look similar to that of (PhO, Cl)-azine and has been omitted.

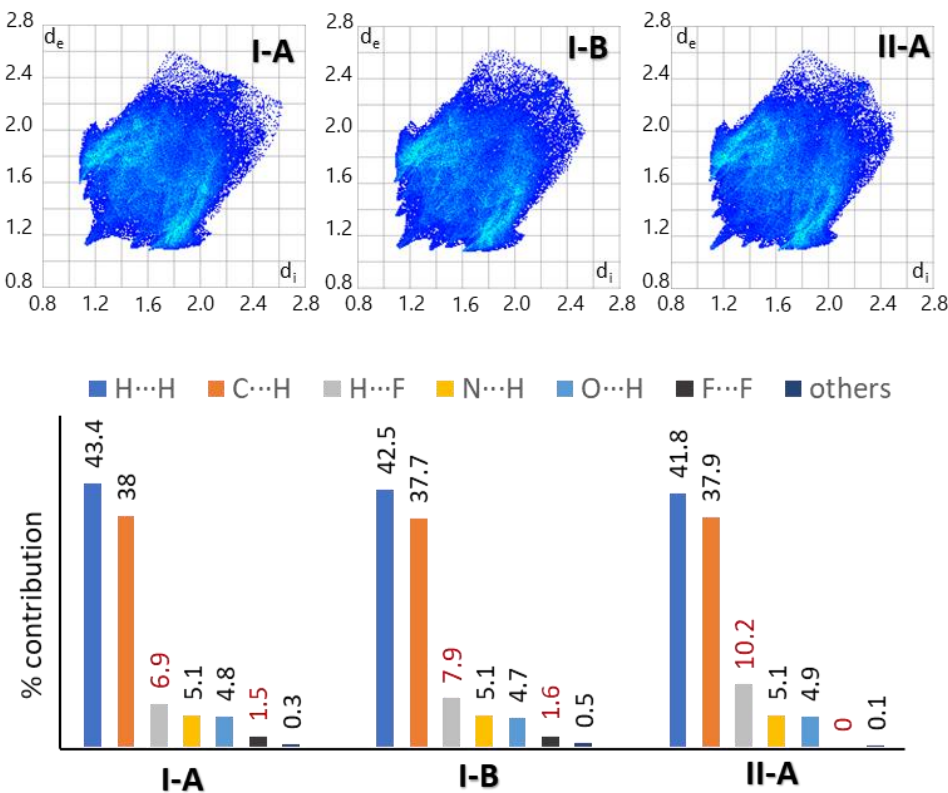
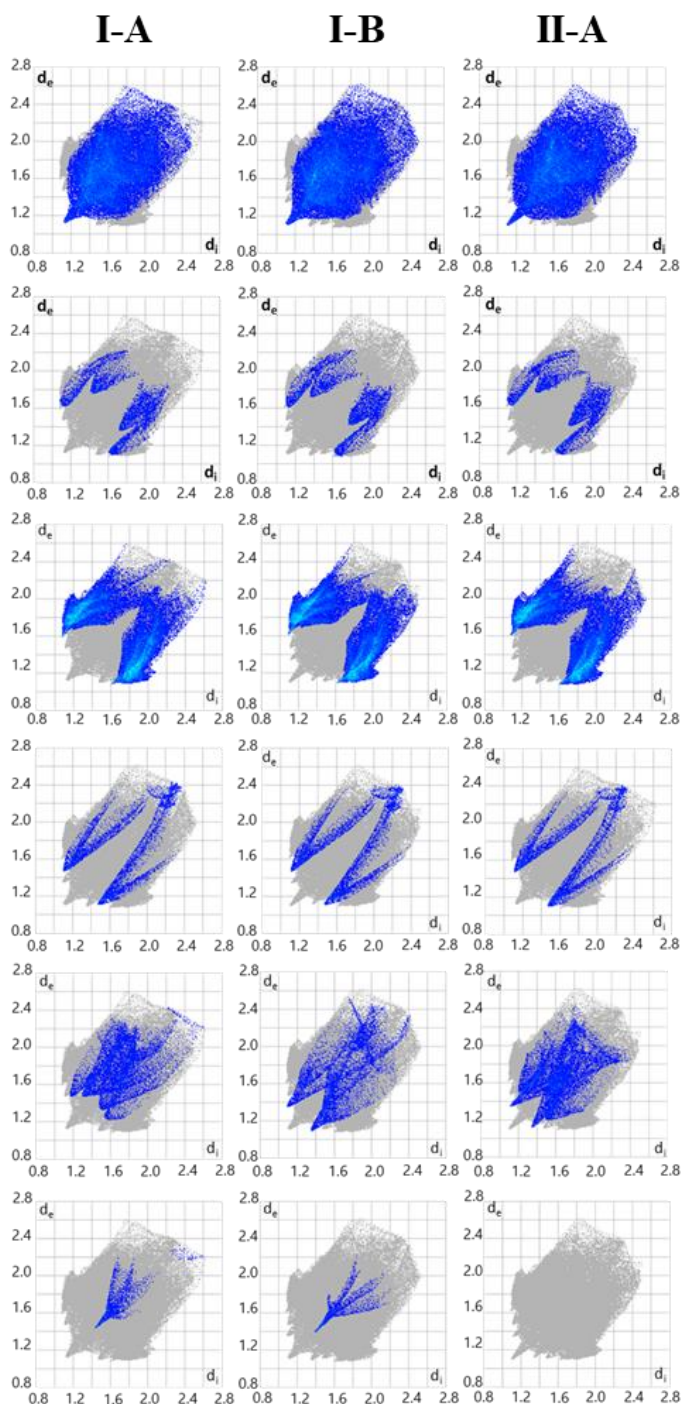


Fig. S13 Hirshfeld fingerprint plots for molecules **I-A**, **I-B**, and **II-A** in polymorphs **I** and **II** (top) and percentage contributions of different types of contacts to the fingerprint plots (bottom). For emphasis, red numbers are used for the interactions most relevant for the current discussion of the significant differences between the polymorphs.



H···H contacts

N···H contacts

C···H contacts

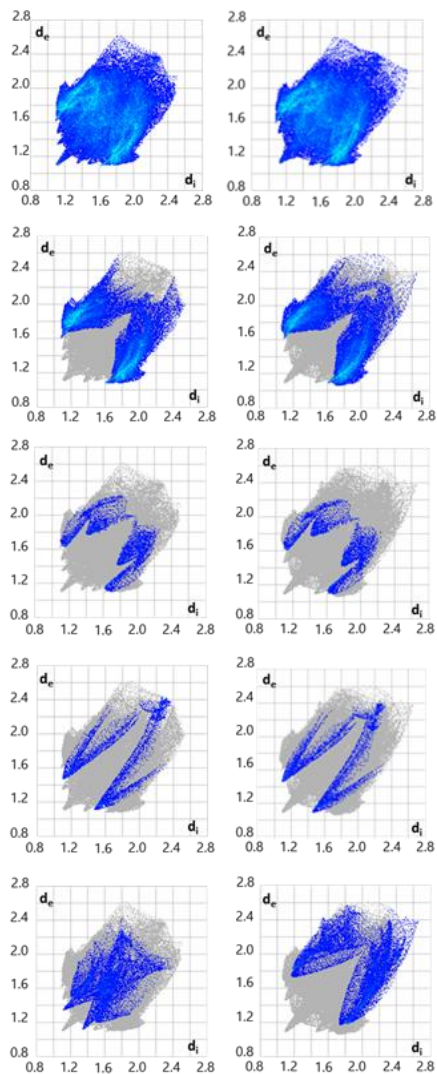
O···H contacts

H···F contacts

F···F contacts

Fig. S14 Hirshfeld fingerprint plots for forms **I-A**, **I-B**, and **II**. The Hirshfeld fingerprint plots were generated using CrystalExplorer, version 21.5. *Interlayer* interactions are shown in red.

(PhO, F)- II (PhO, Cl)



Complete fingerprint plot

C···H contacts

N···H contacts

O···H contacts

H···Halogen contact

Fig. S15 Hirshfeld fingerprint plots for (PhO, F)-azine polymorph **II** and (PhO, Cl)-azine. The plots for the *intralayer* interactions written in black have minimal differences. This means the stabilization of the PBAMs in both the azines result from same types of interactions. The *interlayer* interaction (H···Halogen interaction) exists for the (PhO, F)-azine but not in the case of (PhO, Cl)-azine. This further supports the reasoning for the zigzag pattern in **II**.

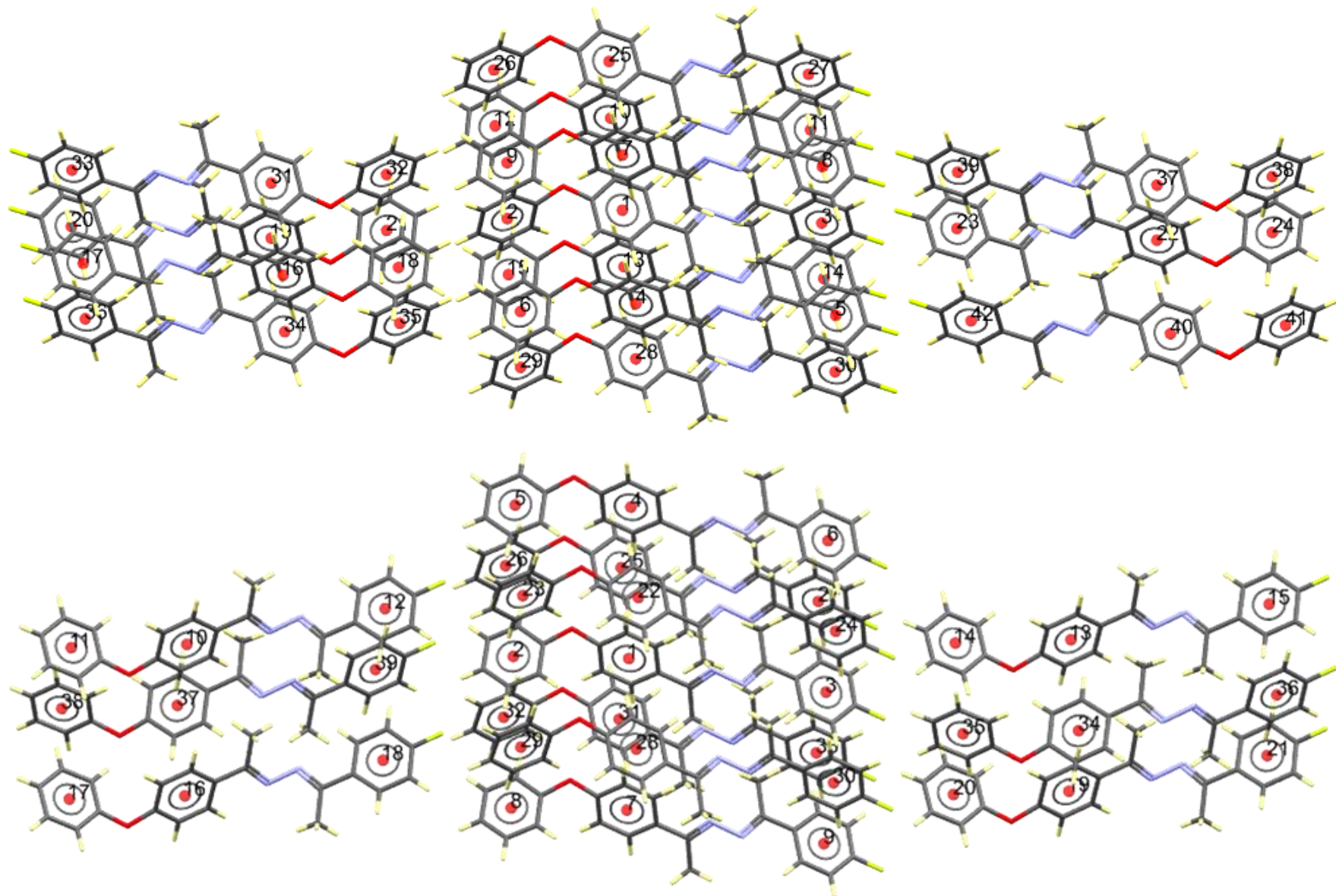


Fig. S16 Molecular packing shells in **I** (top) and **II** (bottom). These neighboring molecules were generated using a default value of van der Waals radii +0.5 Å in the aromatics analyzer tool (CSD-Mercury). Only the arene-arene interactions with a non-zero score are listed for each polymorph in the **Tables S6** and **S7**.

Table S6 Favorable *intralayer* interactions in I

Centroid1	Centroid2	Distance (Ang.)	Orientation (Degrees)	Score ^a
2	6	4.86	74.61	9
2	9	4.85	74.61	9
3	8	4.87	64.72	9
2	12	4.84	74.61	8.9
2	15	4.83	74.61	8.9
3	14	4.81	64.72	8.9
1	7	4.86	62.96	8.8
1	10	4.8	62.96	8.8
1	4	4.9	62.96	8.7
1	13	4.82	62.96	8.7
3	5	4.85	64.72	8.7
3	11	4.85	64.72	8.7
2	32	5.55	0	6.9
3	39	6.25	0	5.1
2	18	6.2	74.61	4.1
2	21	6.2	74.61	4.1
2	35	6.44	0	3.9
1	25	6.54	0	3.7
1	28	6.54	0	3.7
3	27	6.54	0	3.6
3	30	6.54	0	3.6
1	6	6.85	25.55	3.4
2	7	6.88	26.12	3.3
3	23	6.72	64.72	3.3
1	12	6.96	25.55	3
2	26	6.54	0	3
2	29	6.54	0	3
2	13	7	26.12	2.9
1	15	6.81	25.55	1.7
2	10	6.85	26.12	1.7
3	42	7.65	0	1.6
1	9	6.98	25.55	1.5
2	4	7.04	26.12	1.4
1	29	8.08	62.89	0.9
2	25	8.08	62.89	0.9
1	26	8.31	62.89	0.8
2	28	8.31	62.89	0.8
1	11	9.39	2.01	0.4
3	13	9.32	1.63	0.4
1	8	9.42	2.01	0.2
3	4	9.34	1.63	0.2
1	5	10.37	2.01	0.1
1	14	10.33	2.01	0.1
1	27	9.87	64.57	0.1
3	7	10.28	1.63	0.1
3	10	10.27	1.63	0.1
3	28	9.87	64.57	0.1

^aScore between 7-10 represents **strong** interactions that are likely to be significantly stabilising and potentially structure-directing while a score between 5-7 represents **moderate** interactions.

Table S7 Favorable *intralayer* interactions in **II**.

Centroid1	Centroid2	Distance (Ang.)	Orientation (Degrees)	Score ^a
2	29	4.85	72.65	9.1
2	35	4.85	72.65	9.1
2	32	4.84	72.65	9
2	38	4.84	72.65	9
1	28	4.88	63.31	8.9
1	31	4.81	63.31	8.9
1	34	4.88	63.31	8.9
1	37	4.81	63.31	8.9
3	30	4.85	64.87	8.9
3	33	4.84	64.87	8.9
3	36	4.85	64.87	8.9
3	39	4.84	64.87	8.9
2	18	5.85	4.23	6.3
3	20	5.85	4.23	6.3
1	4	6.53	0	3.9
1	7	6.53	0	3.9
3	6	6.53	0	3.8
3	9	6.53	0	3.8
2	5	6.53	0	3.3
2	8	6.53	0	3.3
1	29	6.88	26.13	3.1
2	24	6.63	68.73	3.1
2	34	6.88	26.13	3.1
3	26	6.63	68.73	3.1
1	38	6.96	26.13	2.8
2	12	7.04	4.23	2.8
2	31	6.96	26.13	2.8
3	14	7.04	4.23	2.8
1	32	6.85	26.13	1.7
2	37	6.85	26.13	1.7
1	35	6.98	26.13	1.5
2	28	6.98	26.13	1.5
1	5	8.1	61.72	0.9
2	7	8.1	61.72	0.9
1	8	8.28	61.72	0.8
2	4	8.28	61.72	0.8
1	39	9.33	0.78	0.5
3	31	9.33	0.78	0.5
1	36	9.35	0.78	0.4
3	28	9.35	0.78	0.4
1	9	9.84	64.09	0.3
1	30	10.34	0.78	0.3
1	33	10.33	0.78	0.3
3	4	9.84	64.09	0.3
3	34	10.34	0.78	0.3
3	37	10.33	0.78	0.3

^aScore between 7-10 represents **strong** interactions that are likely to be significantly stabilising and potentially structure-directing while a score between 5-7 represents **moderate** interactions.

Pairwise Interaction Energies

CrystalExplorer Calculations: CE-B3LYP, that is, B3LYP/6-31G(d,p) pairwise interaction energies are computed by generating a cluster of molecules within a radius of 3.8 Å for a selected reference molecule A* in **I**, B* in **I** and A* in **II**. The calculation results in a color-coded interaction energies mapping, **Fig. S17**. The individual energy components electrostatic (E_{ele}), polarization (E_{pol}), dispersion (E_{dis}) and exchange-repulsion (E_{rep}) as well as the sum of energy components (E_{tot}) for the interactions relative to A* are provided in **Table S8**.

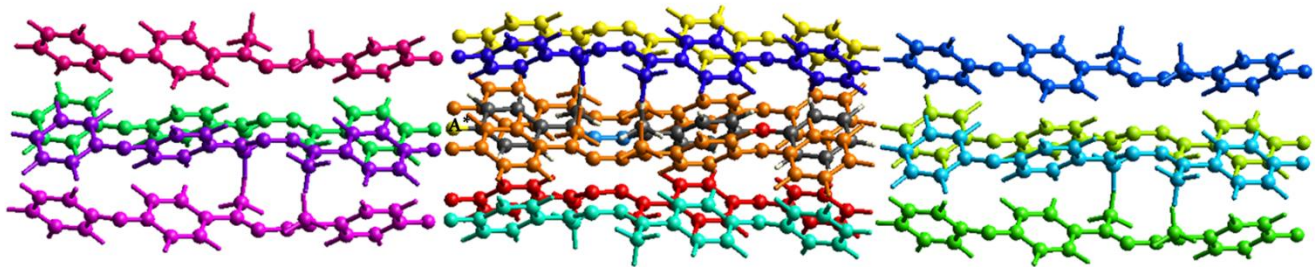


Fig. S17 Color-coded interaction mapping within 3.8 Å of A* in **I**.

Table S8 Color-coded pairwise interaction energies relative to A* in **I**

N ^a	R ^b	E _{ele}	E _{pol}	E _{dis}	E _{rep}	E _{tot}
2	6.54	-4.9	-0.5	-27.5	13.1	-21.4
1	4.86	-20.1	-2.9	-81.5	56.8	-59.2
1	4.84	-19.4	-2.8	-81.5	56.1	-59.0
1	4.84	-16.6	-2.4	-77.5	52.3	-54.5
1	4.84	-16.4	-2.5	-76.9	50.4	-55.0
1	19.78	-0.8	-0.3	-11.4	0	-11.1
1	19.7	-0.9	-0.2	-5.9	0	-6.2
1	19.44	-0.4	-0.3	-4.4	0	-4.4
1	19.59	-1.5	-0.2	-6.8	0	-7.6
1	19.7	-1.1	-0.2	-5.8	0	-6.3
1	18.31	5.7	-0.4	-9.1	0	-2.2
1	19.11	1.1	-0.1	-2.1	0	-0.7
1	18.84	1.9	-0.4	-6.5	0	-4.0

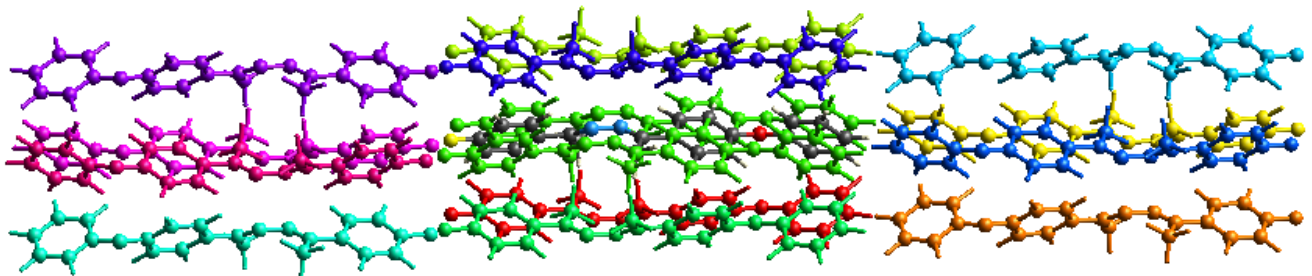


Fig. S18 Color-coded interaction mapping within 3.8 Å of \mathbf{B}^* in **I**.

Table S9 Color-coded pairwise interaction energies relative to \mathbf{B}^* in **I**

N ^a	R ^b	E _{ele}	E _{pol}	E _{dis}	E _{rep}	E _{tot}
2	6.54	-4.9	-0.5	-27.8	13.6	-21.4
1	4.86	-20.1	-2.9	-81.5	56.8	-59.2
1	4.84	-19.4	-2.8	-81.5	56.1	-59
1	4.84	-16.6	-2.4	-77.5	52.3	-54.5
1	4.84	-16.4	-2.5	-76.9	50.4	-55
1	19.7	0	-0.4	-12.1	0	-10.9
1	19.7	0.4	-0.2	-5.9	0	-4.8
1	19.52	1.4	-0.3	-3.9	0	-2.2
1	19.51	-0.4	-0.2	-7.3	0	-6.9
1	19.7	0.5	-0.2	-5.8	0	-4.6
1	18.39	-1.2	-0.7	-11.6	0	-11.9
1	19.11	0.6	-0.1	-2.1	0	-1.2
1	18.84	1.6	-0.4	-6.5	0	-4.3

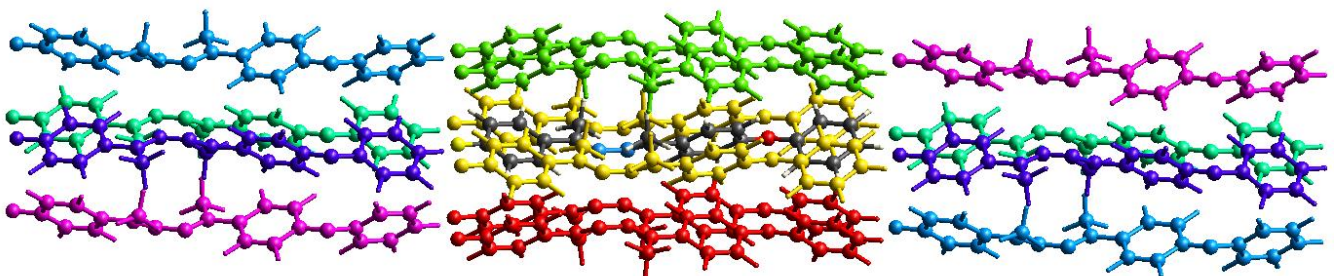


Fig. S19 Color-coded interaction mapping within 3.8 Å of \mathbf{A}^* in **II**.

Table S10 Color-coded pairwise interaction energies relative to \mathbf{A}^* in **II**

N ^a	R ^b	E _{ele}	E _{pol}	E _{dis}	E _{rep}	E _{tot}
2	4.86	-15.9	-2.5	-75.3	48.5	-54.2
2	6.53	-5	-0.5	-28.5	14.1	-21.8
2	4.86	-18.7	-2.7	-79.9	53.4	-58.3
2	18.97	1.7	-0.4	-10.6	0	-7.8
2	19.27	1.2	-0.2	-3.9	0	-2.2
2	19.45	-3.6	-0.4	-5.7	0	-9.1
2	19.27	-0.9	-0.2	-4.3	0	-4.8

Lattice Energy Calculations for Polymorph I and II

CrystalExplorer Calculations: CE-B3LYP, that is, B3LYP/6-31G(d,p) lattice energies are computed by direct summation of pairwise interaction energies in *CrystalExplorer* 21.5 between molecules around a certain distance from the central molecule A. The distance from the central molecule is increased until the lattice energy E_{lat} converges. For the (PhO, F)-azine, convergence of E_{lat} was reached at 25 Å and this distance was chosen as a cut off for all calculations.

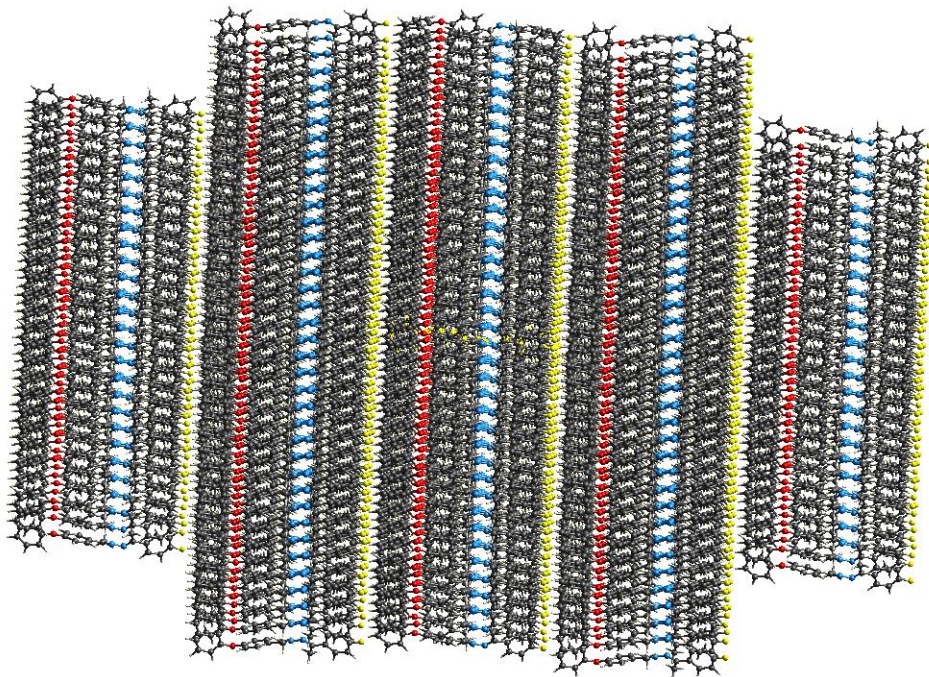


Fig. S20 Molecular packing shell for I used for calculations in *CrystalExplorer* around the central molecule at a distance of 25 Å.

$$\text{The cell dipole energy correction formula: } E_{\text{cell dipole}} = \frac{-2\pi p^2}{3ZV_{\text{cell}}} = -126.13 \frac{(p_{\text{cell}}/D)^2}{Z(V_{\text{cell}}/\text{\AA}^3)} \text{ kJ/mol.}$$

E_{lat} using UNI intermolecular potentials: UNI intermolecular potentials embedded in the CSD-Mercury software are used to estimate the lattice energy of the crystals.

$$\text{Potential} = A \cdot \exp^{(-Br)} - C \cdot r^{(-6)}$$

Unified (UNI) pair-potential parameters:

atom1	code1	atom2	code2	A	B	C
O2	16	O2	16	195309.1	3.74	1335.0
O2	16	N4	23	268571.0	3.86	1523.0
O2	16	F2	6	182706.1	3.98	868.3
O2	16	C26	3	393086.8	3.74	2682.0
O2	16	H26	1	295432.3	4.82	439.3
N4	23	N4	23	365263.0	3.65	2891.0
N4	23	F2	6	249858.9	3.93	1277.9
N4	23	C26	3	491494.0	3.86	2791.0
N4	23	H26	1	228279.0	4.52	502.1
F2	6	F2	6	170916.4	4.22	564.8
F2	6	C26	3	196600.9	3.84	1168.8
F2	6	H26	1	64257.8	4.11	248.4
C26	3	C26	3	226145.2	3.47	2418.0
C26	3	H26	1	120792.1	4.10	472.8
H26	1	H26	1	24158.0	4.01	109.2